

# On the origin of cosmological magnetic fields by plasma instabilities

Reinhard Schlickeiser  
Institut für Theoretische Physik  
Lehrstuhl IV: Weltraum- und Astrophysik  
Ruhr-Universität Bochum, Germany



## Topics:

1. Introduction
2. Cosmological magnetic field generation by the Weibel instability
3. Analytical instability studies
4. PIC simulation
5. Covariant dispersion theory of the Weibel instability
6. Summary

## Collaborators

- P. S. Shukla, U. Schaefer-Rolffs, R. Tautz, M. Lazar (Ruhr-Universität Bochum)
- J.-I. Sakai (Toyama University)

written version: Plasma Physics and Controlled Fusion 47, A205 (2005)



# 1. Introduction:

Today, magnetic fields are present throughout the universe and play an important role in many astrophysical situations.

Our Galaxy and many other spiral galaxies are endowed with coherent magnetic fields ordered on scales  $\geq 10$  kpc with typical strength  $B_G \simeq 3 \cdot 10^{-6} \text{G}$

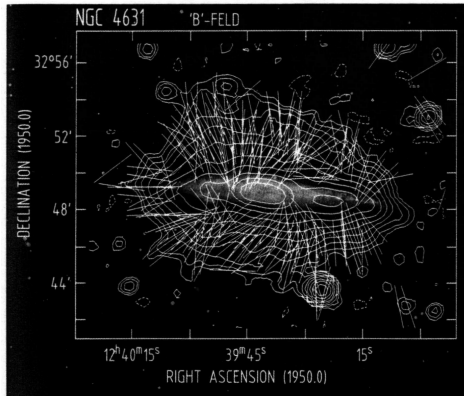


Figure 1: Magnetic field structure in the external edge-on galaxy NGC 4631 derived from radio polarization measurements at  $\lambda = 20\text{cm}$  wavelength by Hummel et al. (1988 [232]), assuming negligible Faraday rotation as indicated by the rotation measures of nearby extragalactic background radio sources



i.e. energy density relative to the cosmic microwave background radiation (CMBR) energy density  $w_\gamma$

$$\Omega_G = (B_G^2/8\pi)/w_\gamma \simeq (B_G/3.2 \cdot 10^{-6}G)^2 \simeq 1 \Omega_\gamma$$

Galactic magnetic field plays a crucial role in the dynamics of the Galaxy: confining cosmic rays and transferring angular momentum away from protostellar clouds so that they can collapse and become stars. Magnetic fields also important in the dynamics of pulsars, white dwarfs, and even black holes.

Elsewhere in the Universe, magnetic fields are known to exist and be dynamically important: in the intracluster gas of rich clusters of galaxies, in quasistellar objects and in active galactic nuclei.

Existence of magnetic fields is a mandatory requirement for the onset of nonthermal phenomena in cosmological sources especially gamma-ray burst sources and relativistic jet sources (e. g. jet formation and collimation by MHD effects, acceleration of charged particles at magnetized shock fronts, synchrotron radiation).

Studying the nonthermal history of our Universe is closely linked to the understanding of the cosmological magnetization process.



The origin of cosmic magnetic fields is not yet known (Grasso and Rubinstein 2001, Kronberg 2002). Many astrophysicists believe that galactic magnetic fields are generated and maintained by dynamo action (Parker 1971) whereby the energy associated with the differential rotation of spiral galaxies is converted into magnetic field energy (Parker 1979, Zeldovich et al. 1983, Rees 1987). **However, the dynamo mechanism is only a means of amplification and dynamos require seed magnetic fields.**

- If a galactic dynamo has operated over the entire age of the galaxy ( $\simeq 10$  Gyr), it could have amplified a tiny seed field of  $\simeq 10^{-19}$  G
- Alternatively, initial fields of strength  $B_c \simeq 10^{-9}$  G can give rise to galactic fields of the observed values without a functioning dynamo mechanism: simple adiabatic compression of magnetic field lines during galaxy formation would amplify such initial fields to the present, observable values.



A primeval magnetic field of  $B_c \simeq 10^{-9}$  G provides an energy density

$$\Omega_B = 10^{-7} \Omega_\gamma (B_c / 10^{-9} \text{G})^2 \quad (1)$$

Since the universe through most of its history has been a good conductor any primeval cosmic magnetic field will evolve conserving magnetic flux  $B_c a^2 \simeq \text{const.}$ , where  $a$  is the cosmic scale factor, implying that the dimensionless ratio  $\Omega_B = (B_c^2 / 8\pi) / w_\gamma$  for homogeneous (uniform or stochastic) magnetic fields remains approximately constant and provides a convenient invariant measure of magnetic field strength.

Naively, from Eq. (1) one would expect a magnetic field of this amplitude to induce perturbations in the CMBR on the order of  $10^{-7}$ , which are about 1 percent of the observed CMBR anisotropies. The absence of such signatures may also serve as a consistency check on models of galaxy evolution that would be observationally incompatible with such large initial fields.



## 2. Cosmological magnetic field generation by the Weibel instability

**Here:** Generation of cosmological seed magnetic fields by the Weibel (1959) instability operating in initially unmagnetised plasmas by colliding ion-electron streams

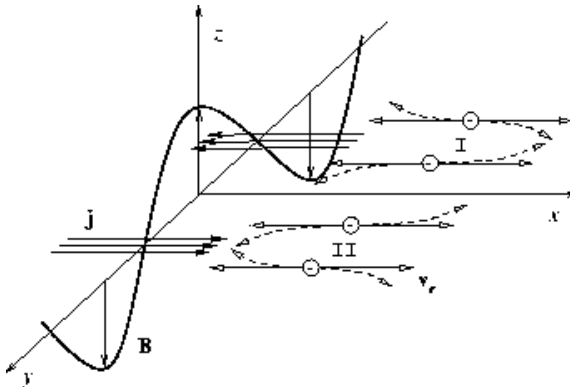


Figure 2: Illustration of the instability. A magnetic field perturbation deflects electron motion along the  $x$ -axis, and results in current sheets ( $\mathbf{j}$ ) of opposite signs in regions I and II, which in turn amplify the perturbation. The amplified field lies in the plane perpendicular to the original electron motion. From Medvedev and Loeb (1999).



## 2.1. Explanation by Fried (1959)

due to counterstreaming electron distributions

$$f_0(\vec{v}) = \delta(v_x^2 - a^2)\delta(v_y)\delta(v_z) = \frac{1}{2}\delta(v_y)\delta(v_z)[\delta(v_x - a) + \delta(v_x + a)]$$

a) electron motion in infinitesimal magnetic fluctuation  $\delta B_z = B_1(t)e^{iky}$

$$\frac{dv_y}{dt} = \frac{e}{m_e c} v_x \delta B_z$$

b) electrons with  $v_x = a \rightarrow \frac{dv_y}{dt} = \frac{ea}{m_e c} \delta B_z$

electrons with  $v_x = -a \rightarrow \frac{dv_y}{dt} = -\frac{ea}{m_e c} \delta B_z$

c) change in total momentum flux in  $x$ -component through surface normal to  $y$ -axis

$$\begin{aligned} \frac{\partial}{\partial t} \langle v_y v_x \rangle &= \int d^3v f_0 v_x \frac{dv_y}{dt} = \frac{e\delta B_z}{2m_e c} \left[ \int_{-\infty}^{\infty} dv_x v_x a \delta(v_x - a) \right. \\ &\quad \left. - \int_{-\infty}^{\infty} dv_x v_x a \delta(v_x + a) \right] = \frac{ea^2 \delta B_z}{m_e c} \end{aligned} \quad (W1)$$





d) this causes a change in  $\langle v_x \rangle$ :

$$\frac{\partial}{\partial t} \langle v_x \rangle = - \frac{\partial \langle v_y v_x \rangle}{\partial y}$$

implying with Eq. (W1)

$$\frac{\partial^2}{\partial t^2} \langle v_x \rangle = \frac{\partial}{\partial y} \frac{\partial \langle v_y v_x \rangle}{\partial t} = - \frac{ea^2}{m_e c} \frac{\partial \delta B_z}{\partial y} = - \frac{ea^2}{m_e c} ik \delta B_z \quad (W2)$$

e) with Ampere law for current

$$j_x = -en_e \langle v_x \rangle = \frac{c}{4\pi} (\text{rot} \vec{B})_x = \frac{c}{4\pi} \frac{\partial \delta B_z}{\partial y} = \frac{c}{4\pi} ik \delta B_z$$
$$\rightarrow \langle v_x \rangle = - \frac{c}{4\pi en_e} ik \delta B_z \quad (W3)$$

insert in Eq. (W2)

$$\frac{\partial^2 \delta B_z}{\partial t^2} = \frac{4\pi e^2 a^2 n_e}{m_e c^2} \delta B_z = \frac{\omega_{p,e}^2 a^2}{c^2} \delta B_z(t)$$

with growing solution

$$\delta B_z(t) \propto \exp\left[\frac{\omega_{p,e} a t}{c}\right]$$



## 2.2. PIC simulation of this situation

Sakai, RS & Shukla 2004, Phys. Lett. A 330, 384)  
2D3V-relativistic PIC simulations ( $m_p/m_e = 64$ )

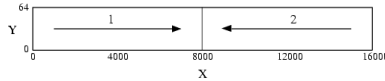


Figure 3: Counter-streaming plasma with system size of  $N_x = 16000$  and  $N_y = 64$ .

**Initial state  $t = 0$ :**

Shifted Maxwellians ( $v_{th,e} = 0.1c$ ,  $T_e = T_p$ , with  $v_{d1} = 0.2c$  and  $v_{d2} = -0.2c$ )

symmetric case: densities  $n_1 = n_2 = 50/\text{cell}$

asymmetric case:  $n_2 = 100/\text{cell} = 2n_1$

no initial electromagnetic fields

electron Debye length  $v_{th,e}/\omega_{pe} = 1.0\Delta$ , collisional skin depth  $c/\omega_{pe} = 10\Delta$  (grid size  $\Delta = 1.0$ )



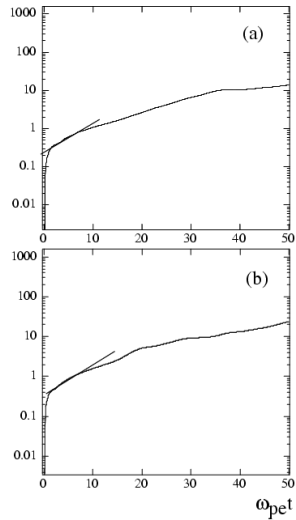


Figure 4: Time evolution of magnetic field energy density  $\int \int B_z^2 dx dy$  during early stage: (a) symmetric case, (b) asymmetric case

Confirms growth of  $B_z$ -component!



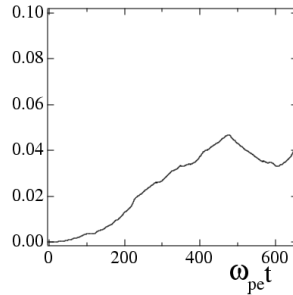


Figure 5: Late time history of the magnetic field energy  $\int \int B_z^2 dx dy$  normalized by the initial electron flow energy.

### 2.3. Origin of plasma streaming

Hydrodynamical simulations of a cold dark matter universe with a cosmological constant  $\neq 0$  are currently most successful theory for cosmological structure formation.

Large-scale structures, such as filaments and sheets of galaxies, evolve by the gravitational collapse of initially overdense regions giving rise to an intense relative motion of fully ionized gaseous matters.



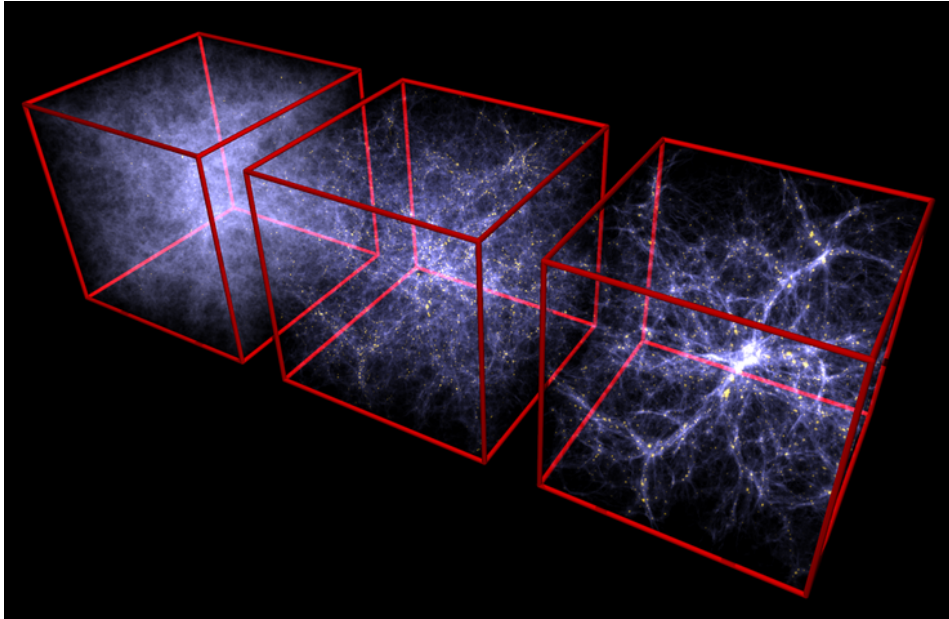


Figure 6: Structure formation in the gaseous component of the universe, in a simulation box 100 Mpc/h on a side. From left to right:  $z=6$ ,  $z=2$ , and  $z=0$ . Formed stellar material is shown in yellow. (courtesy of V. Springel, MPA Garching)



Because sound speed  $c_s = v_{th}/43 \ll v_{th}$ ,  $v_{th} = 1.23 \cdot 10^4 T_7^{1/2}$  km s<sup>-1</sup>,  
→ gaseous shock structures.

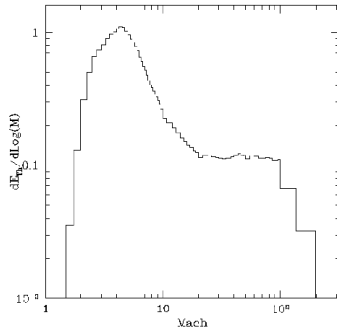


Figure 7: (Miniati 2002)

Extract high Mach number gaseous shock waves: distribution of shocks  
(Miniati 2002)



### 3. Analytical instability studies

#### 3.1. Highly nonlinear problem

charged particles determined by electromagnetic fields:

$$\frac{\partial f_a}{\partial t} + \vec{v} \cdot \frac{\partial f_a}{\partial \vec{x}} + q_a \left[ \vec{E} + \frac{\vec{v} \times \vec{B}}{c} \right] \cdot \frac{\partial f_a}{\partial \vec{p}} = 0$$

electromagnetic fields determined by charged particles:

$$\vec{\nabla} \times \vec{B} - \frac{1}{c} \frac{\partial \vec{E}}{\partial t} = \frac{4\pi}{c} \vec{j}$$

with

$$\vec{j} = \sum_a q_a \int d^3p \vec{v} f_a$$

analytical studies way behind:



(I) mainly linear instability studies in unmagnetized plasmas

$$f_a = f_a^0 + \delta f_a, \vec{B} = \delta \vec{B}$$

Study (Fourier-Laplace analyze) small fluctuations ( $\delta f_a, \delta \vec{B}, \delta \vec{E}$ ) in assumed "quasi-equilibrium" ( $f_a^0$ )

$$\delta f_a \propto e^{-\omega t} = e^{-\omega_R t} e^{\Gamma t}, \Gamma = \Im \omega$$

RS & Shukla 2003, ApJ 599, L57: linear dispersion theory of beam in Maxwellian background;

RS 2004, Phys. Plasmas 11, 5532; Schaefer-Rolffs & RS 2005, Phys. Plasmas 12, 22104: covariant dispersion theory of linear waves in bi-Maxwellian plasma;

Tautz & RS 2005, Phys. Plasmas, submitted: covariant dispersion theory of linear waves in counterstreaming Maxwellian plasmas

plus

**II. educated guesses on intermediate relaxation processes**





## 3.2. Sequence of time evolution

Start from initial counterstreaming distribution in appropriate frame of reference

$$f_a^0(t=0) = C_a \exp\left[-\frac{v_x^2 + v_y^2}{w_{a,th}^2}\right] \left[ \epsilon \exp\left[-\frac{(v_z - v_0)^2}{w_{a,z}^2}\right] + \epsilon' \exp\left[-\frac{(v_z + v_0)^2}{w_{a,z}^2}\right] \right]$$

Relaxes first with respect to longitudinal electrostatic waves to plateau ( $\frac{\partial f_a}{\partial v_z} = 0$ ) in streaming  $v_z$ -direction

→ Intermediate bi-Maxwellian distribution ( $v_{\parallel} = v_z, v_{\perp}^2 = v_x^2 + v_y^2$ )

$$f_a^0(t=t_L) = N_a \exp\left[-\frac{v_{\perp}^2}{w_{a,th}^2} - \frac{v_{\parallel}^2}{v_0^2}\right]$$

is Weibel unstable with respect to aperiodic ( $\omega_R = 0, \Gamma > 0$ ) transverse electromagnetic fluctuations at scales  $(c/\omega_{p,e}) \leq l \leq L_0$  if  $v_0 > w_{th,e}$



Weibel instability threshold corresponds in equal temperature proton-electron plasma to  $v_0 > 43c_S$

If regions of intense streaming are characterized by hydrodynamic shock waves (cosmological baryonic simulations) Weibel instability threshold corresponds to Mach numbers

$$M_{th} > 43$$

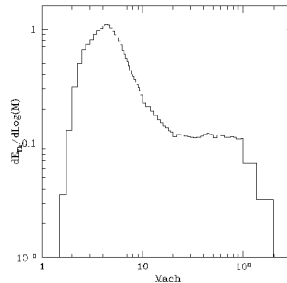


Figure 8: (Miniati 2002)

- expect simultaneous presence of electrostatic waves
- Weibel instability occurs as a secular instability after full development the Langmuir instability



This distribution corresponds exactly to case studied by Weibel: (apart from change of notation: now  $\parallel$  corresponds to  $k_{\parallel}$ ) in the limit  $v_0 > w_{th,e}$ , the dispersion relation reads

$$\omega^4 - (\omega_{p,e}^2 + k^2 c^2)\omega^2 - \omega_{p,e}^2 v_0^2 k^2 = 0$$

Implies purely growing modes with the growth rate

$$\Gamma \simeq \frac{v_0 \omega_{p,e} k}{(\omega_{p,e}^2 + k^2 c^2)^{1/2}}$$

with wavenumbers restricted to

$$k < k_{s,max} = v_0 \omega_{p,e} / (v_{th} c)$$

so that maximum growth rate is

$$\Gamma_{max} = \frac{v_0 \omega_{p,e}}{c} = 0.54 n_{-4}^{1/2} T_7^{1/2} M \text{ s}^{-1}$$

→ minimum growth time of the secular Weibel instability  $\tau_s = \Gamma_{max}^{-1}$  much smaller than any cosmological time scale!



### 3.3. Estimate of saturated magnetic field value

(see also discussion by Kato 2005, astro-ph 0501110)

Free streaming of particles across the magnetic field lines is suppressed once the magnetic field amplitude has grown to a level that the particle's gyroradii in the excited magnetic fields, viz.  $\rho = v_0/\Omega_e$ , are comparable to the characteristic scale length of unstable modes,  $k_{s,\max}^{-1}$ , yielding

$$B \simeq \frac{m_e v_0 c k_{s,\max}}{e} = \sqrt{4\pi n_e m_e} \frac{v_0^2}{v_{th}}$$

Condition can be rewritten as

$$\frac{B^2/8\pi}{n_e m_e v_0^2} = \frac{v_0^2}{2v_{th}^2}$$

Computer simulations of the instability (Califano et al. 1998, Kazimura et al. 1998, Yang et al. 1994, Wallace & Epperlein 1991) confirm that saturation occurs at slightly subequipartition values of  $B$ ,

$$\frac{B_s^2/8\pi}{n_e m_e v_0^2} = \eta \frac{v_0^2}{2v_{th}^2}$$

with  $\eta \simeq 0.01 - 0.1$ . Using  $\eta = 0.01$

$$B_s \simeq 0.1 \sqrt{4\pi n_e m_e} \frac{m_e}{m_p} v_{th} M^2 = 1.3 \times 10^{-7} T_7^{1/2} \left(\frac{M}{43}\right)^2 \text{ G}$$



Consequently, the secular Weibel instability provides saturated magnetic field values over a rather wide range being determined by the distribution of Mach numbers of shock waves from cosmological structure formation with values larger than the instability condition  $M > 43$ .

Taking  $M = 100$  as upper limit, the **maximum field strength** is  $B_{s,max} \simeq 7.0 \cdot 10^{-7} \text{ G}$ .

Consistent with the upper limit  $\leq 10^{-6} \text{ G}$  in large-scale filaments and sheets, derived from rotation measure observations (Rye et al. 1998).

Viable alternative mechanism to all Biermann battery-type processes !



## 4. PIC simulation

(Sakai, RS & Shukla 2004, Phys. Lett. A 330, 384)  
2D3V-relativistic PIC simulations ( $m_p/m_e = 64$ )

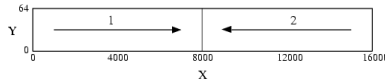


Figure 9: Counter-streaming plasma with system size of  $N_x = 16000$  and  $N_y = 64$ .

**Initial state**  $t = 0$ :

Shifted Maxwellians ( $v_{th,e} = 0.1c$ ,  $T_e = T_p$  with  $v_{d1} = 0.2c$  and  $v_{d2} = -0.2c$ )

symmetric case: densities  $n_1 = n_2 = 50/\text{cell}$

asymmetric case:  $n_2 = 100/\text{cell} = 2n_1$

no initial electromagnetic fields

electron Debye length  $v_{th,e}/\omega_{pe} = 1.0\Delta$ , collisional skin depth  $c/\omega_{pe} = 10\Delta$  (grid size  $\Delta = 1.0$ )



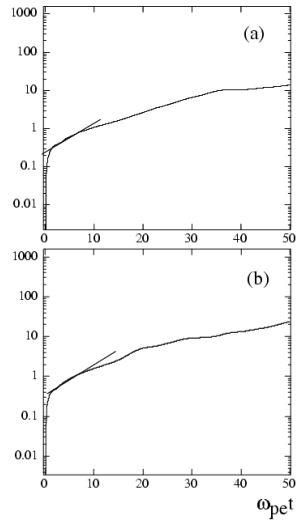


Figure 10: Time evolution of magnetic field energy density  $\int \int B_z^2 dx dy$  during early stage: (a) symmetric case, (b) asymmetric case

Good agreement of linear growth rate with analytical estimate!



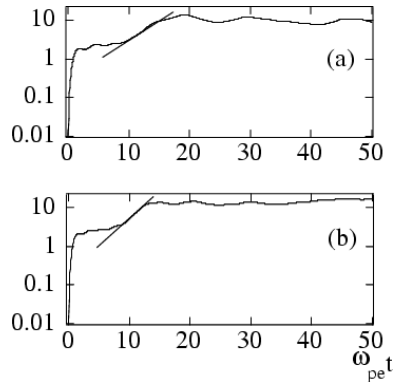


Figure 11: Time evolution of longitudinal electrostatic field energy  $\iint E_x^2 dx dy$  during early stage: (a) symmetric case, (b) asymmetric case

Confirms simultaneous generation of electrostatic waves with good agreement of linear growth rate with analytical estimate





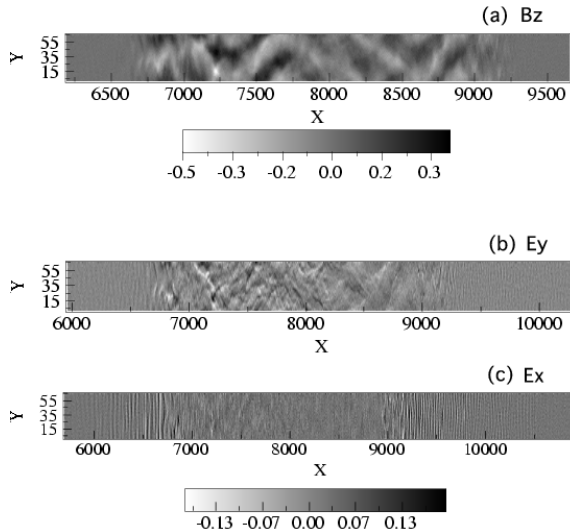


Figure 12: The spatial distributions at  $\omega_{pe}t = 600$  for the asymmetric case: (a) transverse magnetic field component  $B_z$ , (b) transverse electric field component  $E_y$ , (c) longitudinal electric field component  $E_x$



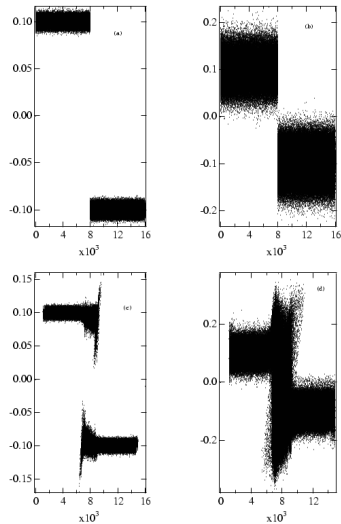


Figure 13: Phase-space plots of the protons  $V_{ix}/c$ , (a)  $\omega_{pe}t = 0$ , (c)  $\omega_{pe}t = 600$ , and the electrons  $V_{ex}/c$ , (b)  $\omega_{pe}t = 0$ , (d)  $\omega_{pe}t = 600$ .



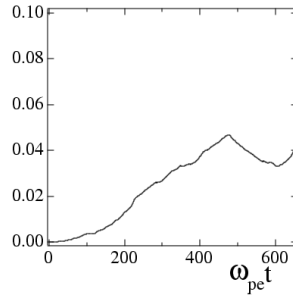


Figure 14: Time history of the magnetic field energy  $\int \int B_z^2 dx dy$  normalized by the initial electron flow energy.

Indicates values  $\eta = 0.05$  of subequipartition parameter for  $u/c = v_0/c = 0.2$ . Analytical estimate with  $\eta = 0.01$  was very conservative!



## 5. Covariant dispersion theory of the Weibel instability

(RS 2004, Phys. of Plasmas 11, 5532)

Existing analytical treatments of the linear Weibel instability have been based on the linearized **nonrelativistic** Vlasov equation, where nonrelativistic particle momentum  $p = mv$ , which neglects the additional Lorentz factor dependence  $p = \gamma mv$  where

$$\gamma = \sqrt{1 + \frac{p^2}{m^2 c^2}} \quad (2)$$

Consider anisotropic bi-Maxwellian equilibrium distributions characterized by the two parameters  $\mu_a = m_a c^2 / k_B T_\perp$  and  $\psi_a$  which in the nonrelativistic limit  $\mu_a \gg 1$  correspond to the perpendicular thermal velocity  $v_{th,a,\perp} = c\sqrt{2/\mu_a}$  and the temperature anisotropy  $\psi_a = \frac{1}{2}[\frac{T_{a,\perp}}{T_{a,\parallel}} - 1]$ .

In the limit of nonrelativistic ( $\mu_a \gg 1$ ) anisotropic plasmas express the transverse dispersion relation in terms of Fried and Conte (1961) plasma dispersion function

$$Z(f) = \frac{1}{\pi^{1/2}} \int_{-\infty}^{\infty} dx \frac{e^{-x^2}}{x - f} \quad (3)$$





$$0 = \Lambda_T \simeq 1 - \frac{c^2 k^2 + \sum_a \omega_{p,a}^2}{\omega^2} - \frac{1}{2} \sum_a \frac{\omega_{p,a}^2}{\omega^2} \left[ 1 + \frac{2\psi_a}{1 - z^2} \right] Z'(f) \quad (4)$$

where  $z = \omega/kc$ ,  $Z'(f) = dZ/df$  and

$$f = \frac{\omega}{v_{th,a,\parallel} k} \frac{1}{\sqrt{1 - \frac{\omega^2}{k^2 c^2}}} \quad (5)$$

In the formal limit of an infinitely high speed of light  $c \rightarrow \infty$  this dispersion relation reduces to the standard noncovariant nonrelativistic form

$$0 = \Lambda_{T,\infty} \simeq 1 - \frac{c^2 k^2 + \sum_a \omega_{p,a}^2}{\omega^2} - \frac{1}{2} \sum_a \frac{\omega_{p,a}^2}{\omega^2} [1 + 2\psi_a] Z'(f_\infty) \quad (6)$$

where

$$f_\infty = \frac{\omega}{v_{th,a,\parallel} k} \quad (7)$$

## 5.1. Aperiodic solutions

(Schaefer-Rolffs & RS, 2005, Phys. of Plasmas 12, 22104)

purely growing ( $\omega = i\Omega$ ) solutions

with  $\omega_0^2 = \sum_a \omega_{p,a}^2$ ,  $\gamma = v_{th,\parallel}/v_{th,\perp}$  (same anisotropy factor for all species)

→ covariant dispersion relation

$$G\left(\frac{\Omega}{v_{th,\parallel}k} \frac{1}{\sqrt{1 + \frac{\Omega^2}{k^2c^2}}}\right) = \frac{k^2c^2 + \Omega^2}{\frac{k^2c^2}{\gamma^2} + \Omega^2} \left[1 + \frac{k^2c^2}{\omega_0^2} + \frac{\Omega^2}{\omega_0^2}\right] \quad (8)$$

with

$$G(y) = 1 - \pi^{1/2} y e^{y^2} \operatorname{erfc}(y), \quad 0 \leq G(y) \leq 1, \quad \forall y \geq 0$$

limit  $c \rightarrow \infty$  of Eq. (8) yields noncovariant dispersion relation

$$G\left(\frac{\Omega}{v_{th,\parallel}k}\right) = \gamma^2 \left[1 + \frac{k^2c^2}{\omega_0^2} + \frac{\Omega^2}{\omega_0^2}\right] \quad (9)$$

discussed by Kalman, Montes & Quemeda (1968, Phys. Fluids 11, 1797)



- Dispersion relations (8) and (9) provide basically identical solutions  $\Omega(k)$ .
- Covariant modifications play no significant role for nonrelativistic plasma temperatures.

with  $\alpha = v_{th,\parallel}/c$ , dimensionless wavenumber  $\kappa^2 = \frac{k^2 c^2}{\omega_0^2}$

and

$$x = \frac{\Omega^2}{k^2 c^2} = \frac{\Omega^2}{\omega_0^2 \kappa^2} \in [0, \infty]$$

→ noncovariant dispersion relation

$$G\left(\frac{\sqrt{x}}{\alpha}\right) = R(x) = \gamma^2[1 + \kappa^2(1 + x)] \quad (10)$$

→ covariant dispersion relation

$$\begin{aligned} G\left(\frac{1}{\alpha} \sqrt{\frac{x}{1+x}}\right) &= S(x) \\ &= \frac{\gamma^2[1 + \kappa^2(1 + x)](1 + x)}{1 + \gamma^2 x} = R(x) \frac{1 + x}{1 + \gamma^2 x} \end{aligned} \quad (11)$$



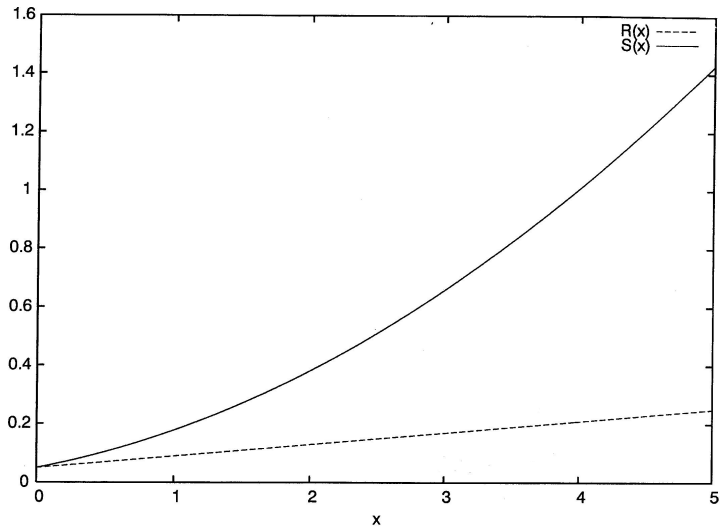


Figure 11: The dispersion functions  $R(x)$  and  $S(x)$  as a function of the dimensionless growth rate  $x$  calculated for  $\gamma = 0.1$  and  $\kappa = 2$ .





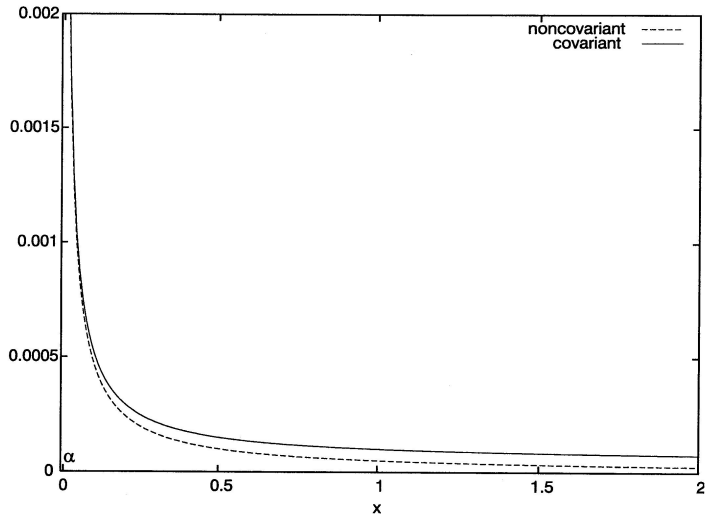


Figure 12: Variation of the covariant function  $G(\sqrt{x/(1+x^2)})/\alpha$  and thenoncovariant function  $G(\sqrt{x}/\alpha)$  as a function of the dimensionless growth rate  $x$  for the case  $\alpha = 0.01$ .



- only aperiodic solutions for  $\alpha \ll \gamma < 1$  (i.e.  $c \gg v_{th,\perp} > v_{th,\parallel}$ )
- no solutions with  $x \geq 1$  possible because for  $x > 1$

$$G(\alpha^{-1} \sqrt{\frac{x}{1+x}}) \rightarrow G(\alpha^{-1}) \simeq \alpha^2/2$$

and  $S(x \geq 1) > \gamma^2 \gg \alpha^2$

- in relevant solution range  $x \leq 1$  covariant function  $S(x)$  and noncovariant function  $R(x)$  approach same limit

$$S(x \leq 1) \simeq R(x \leq 1) \simeq \gamma^2(1 + \kappa^2) = \frac{1 + \kappa^2}{1 + \kappa_{\max}^2}$$

where  $\kappa_{\max}^2 = (1 - \gamma^2)/\gamma^2$

- practically no difference between covariant and noncovariant solutions



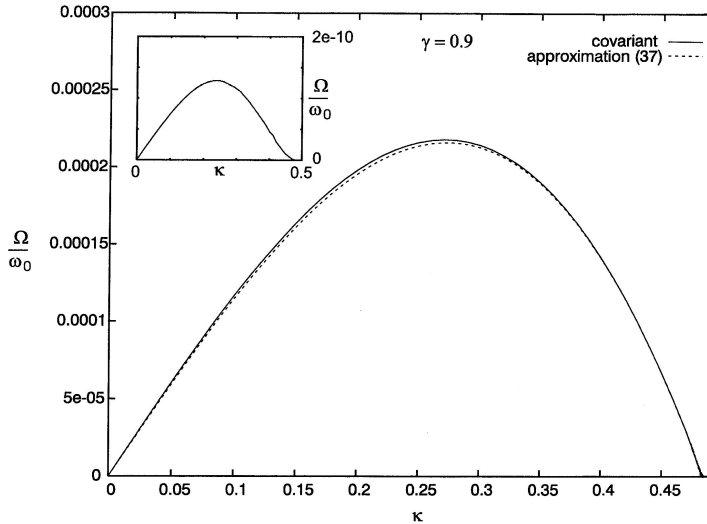


Figure 13: The growth rate  $\Omega/\omega_0$  for  $\gamma = 0.9$  with the analytical approximation (37). Inserted is the difference between the two numerical solutions.



## 6. Summary

- counterstreaming electron-ion plasmas induced by cosmological structure formation magnetize the early universe by Weibel-type instabilities
- intense streaming velocities required  $u > v_{th}$  or  $M > 43$
- good agreement between PIC simulations ( $m_p/m_e = 64$ ) and analytical noncovariant instability estimates
- saturated magnetic fields 5 percent of initial flow energy
- for nonrelativistic thermal velocities practically no difference between covariant and noncovariant plasma dispersion theory

